



Supplement of

Updated climatological mean $\Delta f\text{CO}_2$ and net sea–air CO_2 flux over the global open ocean regions

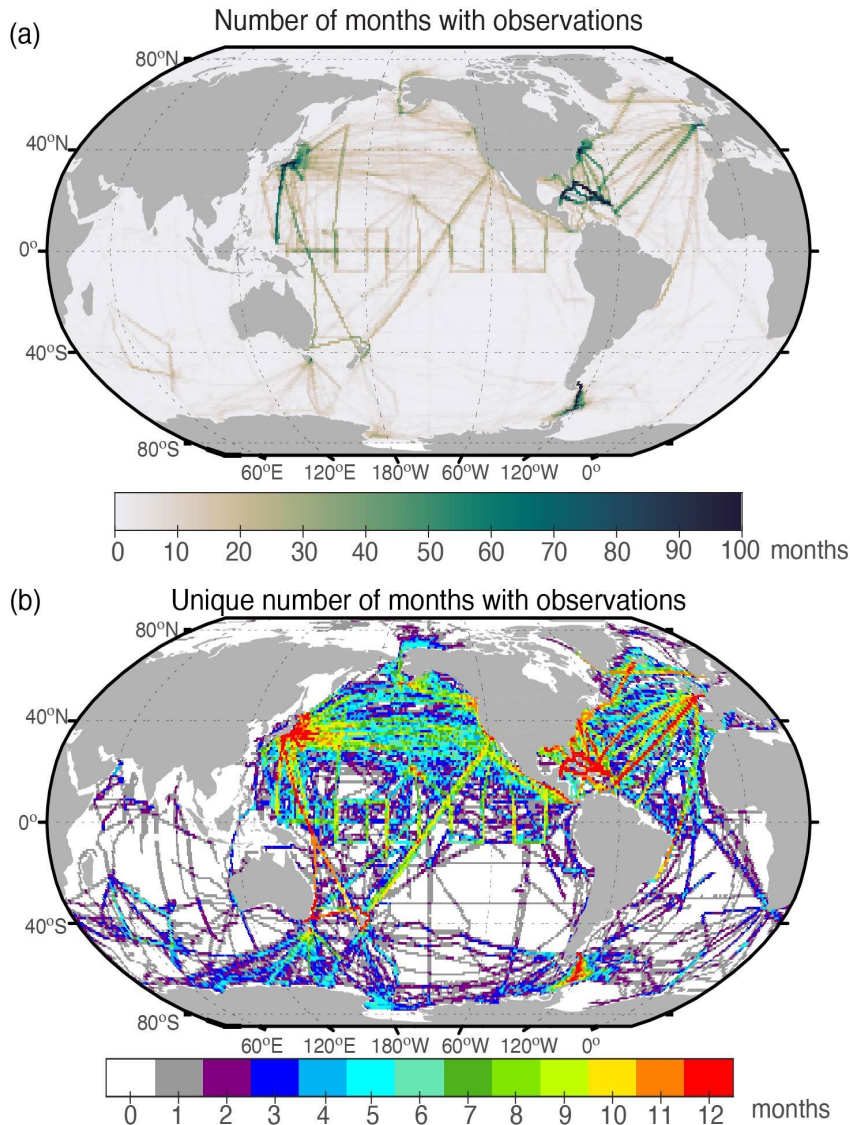
Amanda R. Fay et al.

Correspondence to: Amanda R. Fay (afay@ldeo.columbia.edu)

The copyright of individual parts of the supplement might differ from the article licence.

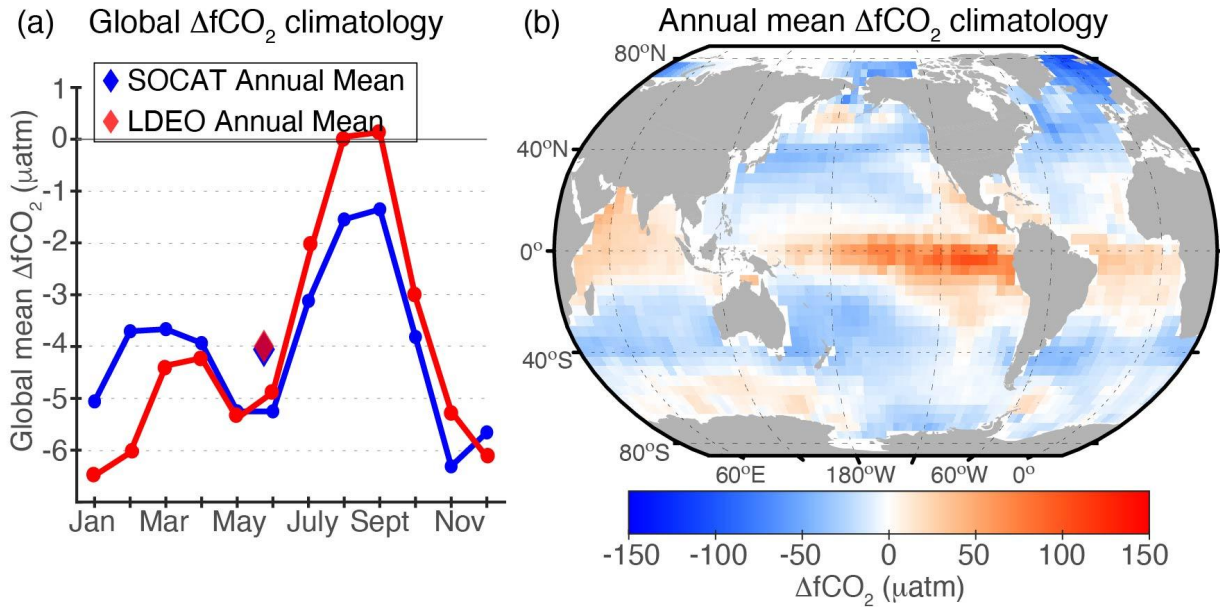
1 Supplementary Figures

2
3



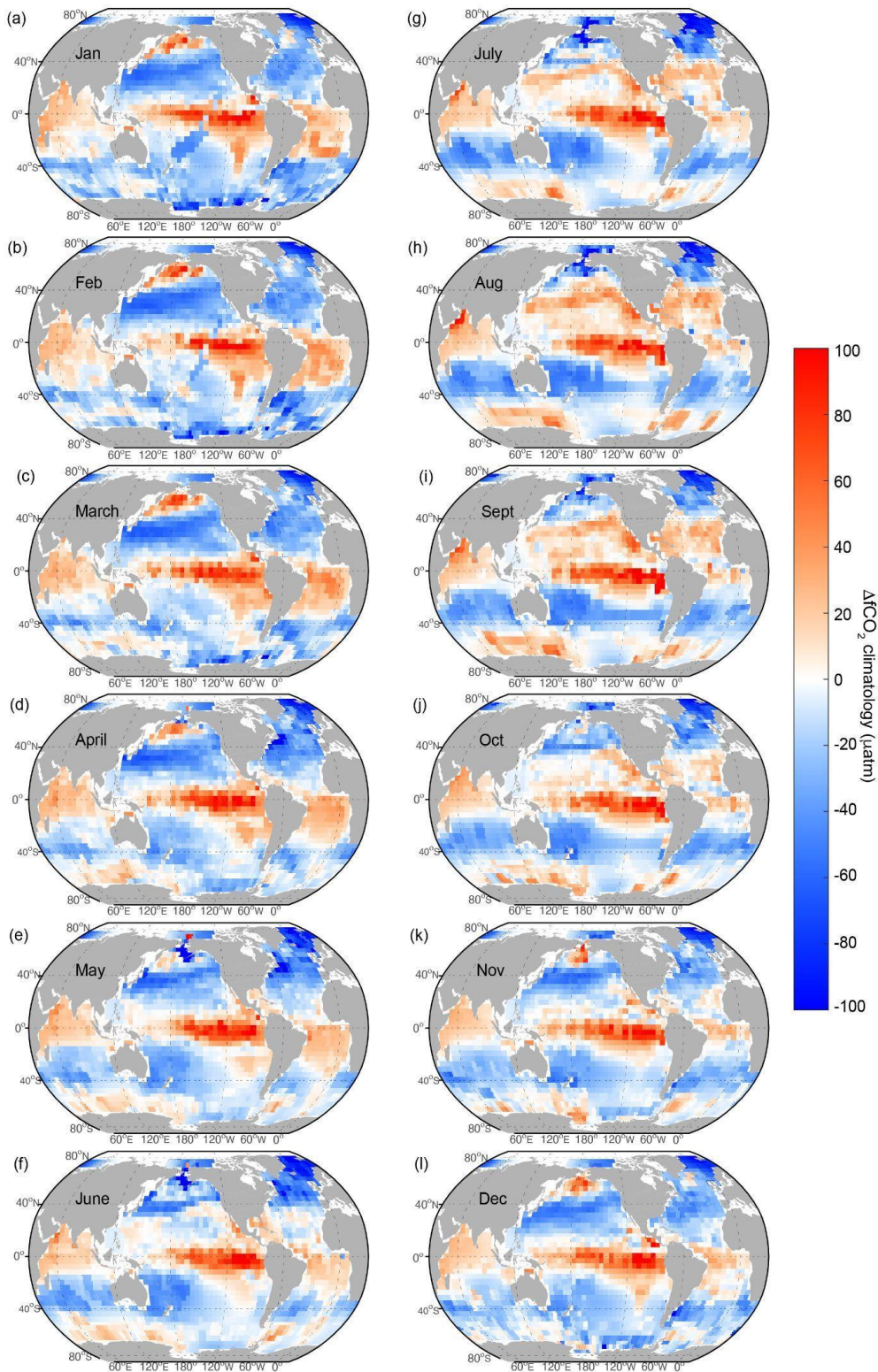
4
5 Figure S1: (a) Total number of months with at least one observation in each 1° grid cell
6 in the LDEOV2019 database, for years 1980-2019. The maximum number possible for a
7 grid cell is 480 (40 years * 12 months). (b) the number of unique calendar months in
8 each grid cell where at least one observation has been made since 1980. Red indicates
9 grid cells where each month (Jan - Dec) has been sampled at least once over the 40
10 year time series while white indicates grid cells with no measurements over the length
11 of the time series.

12
13



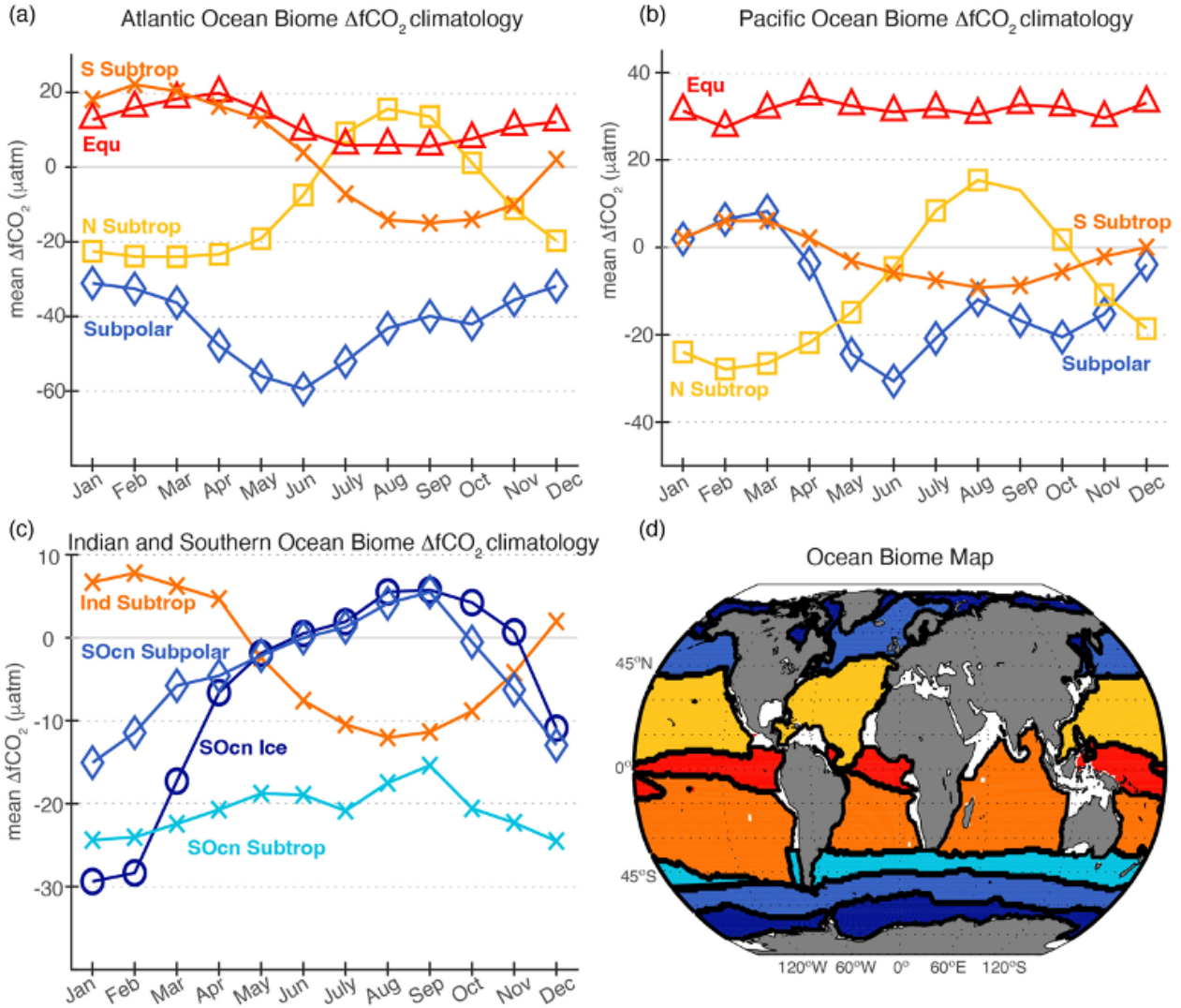
14
 15 Figure S2: (a) Global mean delta fCO₂ seasonal climatology from the SOCATv2022
 16 (blue) and LDEOv2019 (red) databases; annual mean values are indicated by the
 17 diamond (SOCATv2022 = -4.1 μatm and LDEOv2019 = -3.9 μatm). (b) Map of annual
 18 $\Delta f\text{CO}_2$ climatology using LDEOv2019 database.

19
 20
 21
 22



23
 24 Figure S3. Monthly mean values for sea–air $\Delta f\text{CO}_2$ obtained using the LDEO database.
 25 Warm colors indicate positive $\Delta f\text{CO}_2$ (ocean is greater than atmospheric CO_2), white
 26 indicates near zero $\Delta f\text{CO}_2$, and cool colors indicate negative $\Delta f\text{CO}_2$ (ocean CO_2 is lower
 27 than the atmosphere).

28
29
30

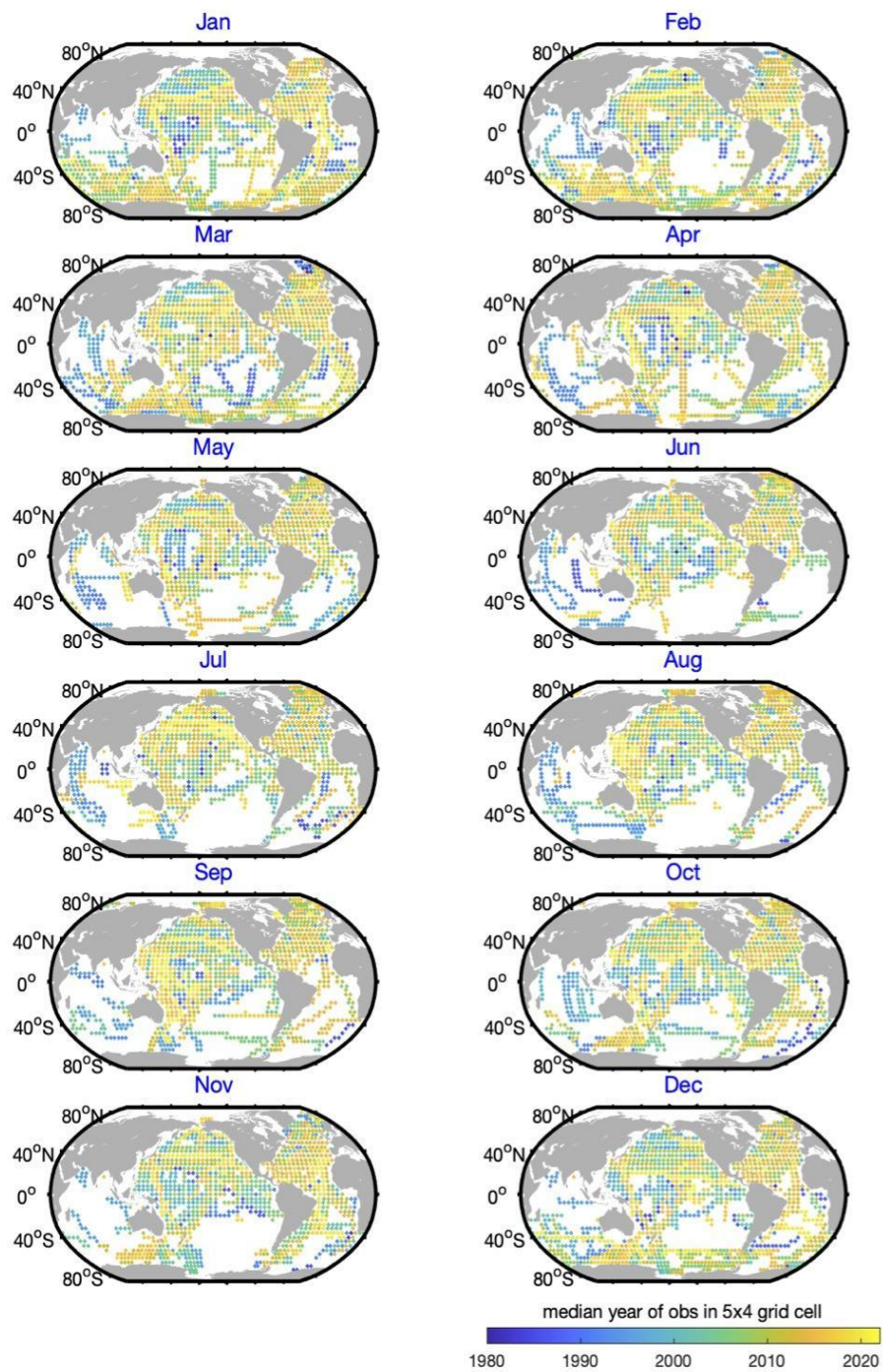


31
32 Figure S4: Monthly climatology (produced using the LDEO database) of ΔfCO_2 for each
33 regional ocean biome in the (a) Atlantic, (b) Pacific, (c) Indian and Southern Ocean
34 basins. (d) Map of regional biomes. Colors of curves correspond to regions on the map
35 in (d) with labels in matching colored text. Note that the y-axis varies between subplots.
36

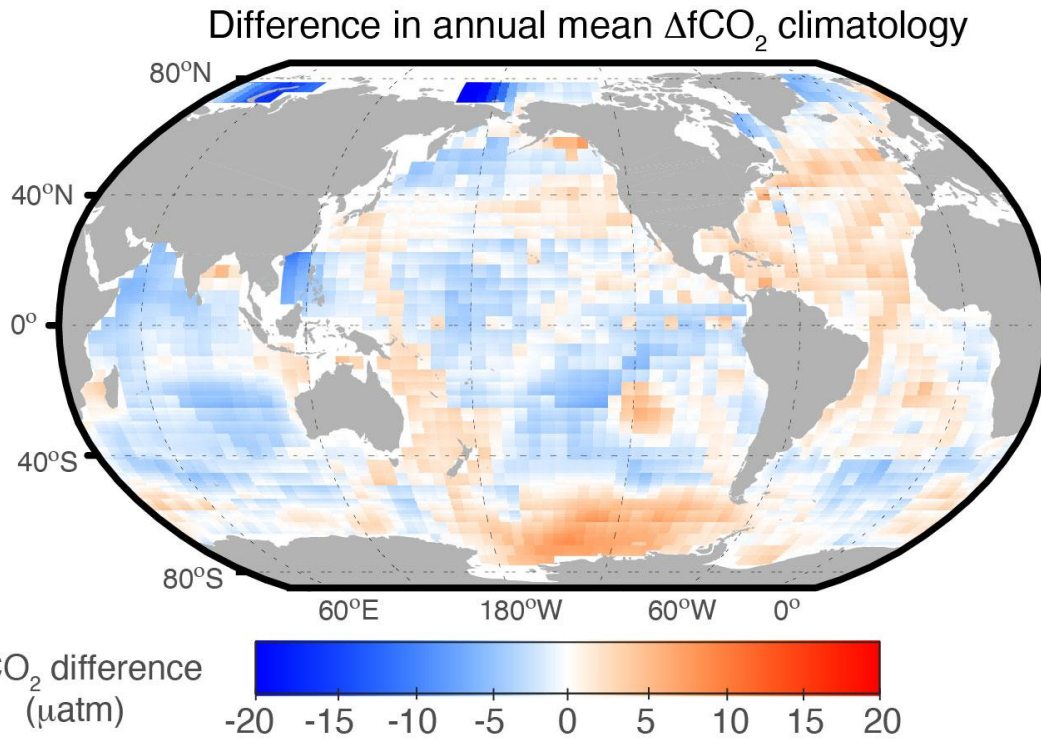
Biome	DJF	MAM	JJA	SON
NP ICE	None (1)	-18.27 (3)	0.64 (20)	1.65 (20)
NP SPSS	2.1 (29)	0.99 (36)	0.94 (38)	1.76 (33)
NP STSS	1.62 (41)	1.38 (37)	1.78 (35)	2.05 (34)
NP STPS	1.49 (41)	1.45 (38)	2.14 (38)	1.94 (36)
W Pac Equ	1.36 (41)	1.38 (34)	1.64 (35)	1.75 (36)
E Pac Equ	2.57 (38)	1.97 (37)	2.04 (34)	2.36 (34)
SP STPS	1.06 (36)	0.54 (36)	0.45 (35)	0.41 (35)
NA ICE	1.38 (12)	0.42 (17)	1.92 (19)	1.82 (20)
NA SPSS	2.02 (27)	1.5 (32)	1.58 (32)	1.28 (31)
NA STSS	1.83 (29)	1.71 (30)	2.08 (31)	1.91 (34)
NA STPS	1.57 (30)	1.59 (28)	2.04 (28)	1.78 (34)
Atl Equ	1.37 (18)	1.49 (23)	1.41 (17)	1.71 (26)
SA STPS	1.69 (24)	1.88 (20)	1.64 (15)	1.58 (27)
IND	1.49 (29)	1.89 (17)	2.23 (17)	1.64 (14)
SO STSS	1.82 (34)	1.69 (32)	1.37 (32)	1.13 (33)
SO SPSS	1.67 (34)	1.77 (32)	1.88 (29)	1.71 (32)
SO ICE	0.87 (33)	1.00 (28)	1.77 (25)	2.64 (29)

38

39 Table S1: Seasonal trends ($\mu\text{atm/yr}$) for biome-mean $f\text{CO}_2$ values- rows representing
40 the 17 biomes as described in Fay & McKinley et al. 2014 and columns representing
41 seasons (DJF: December, January, February; MAM: March, April, May, etc). Value in
42 parentheses in each cell indicates the number of years with a biome mean value
43 available in that season (max would be 42 as there are 42 years included in our
44 analysis of 1980-2021).

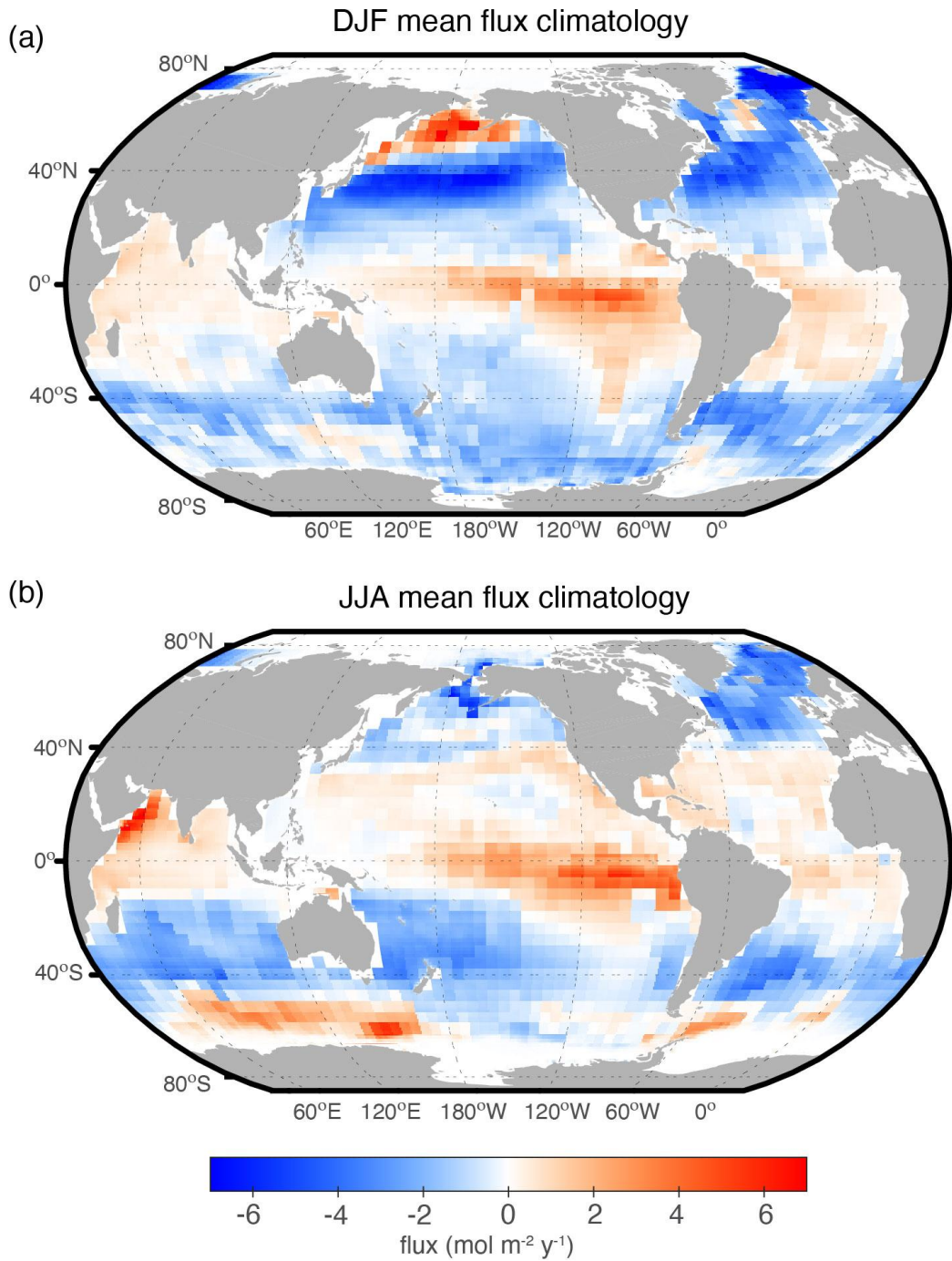


45
 46 Figure S5: Median year of all observations feeding into this climatology, mapped for
 47 each month.

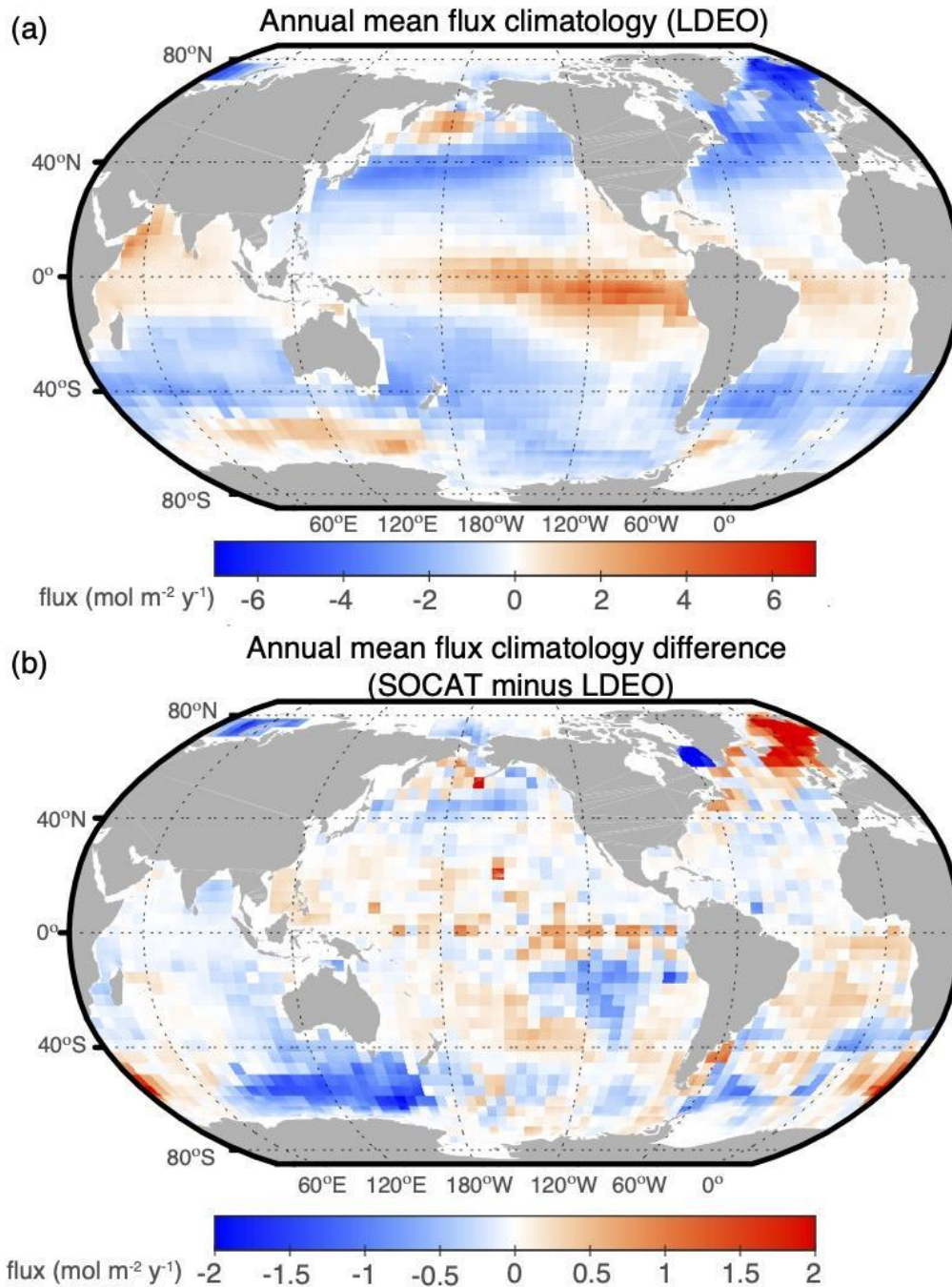


48
49
50
51
52

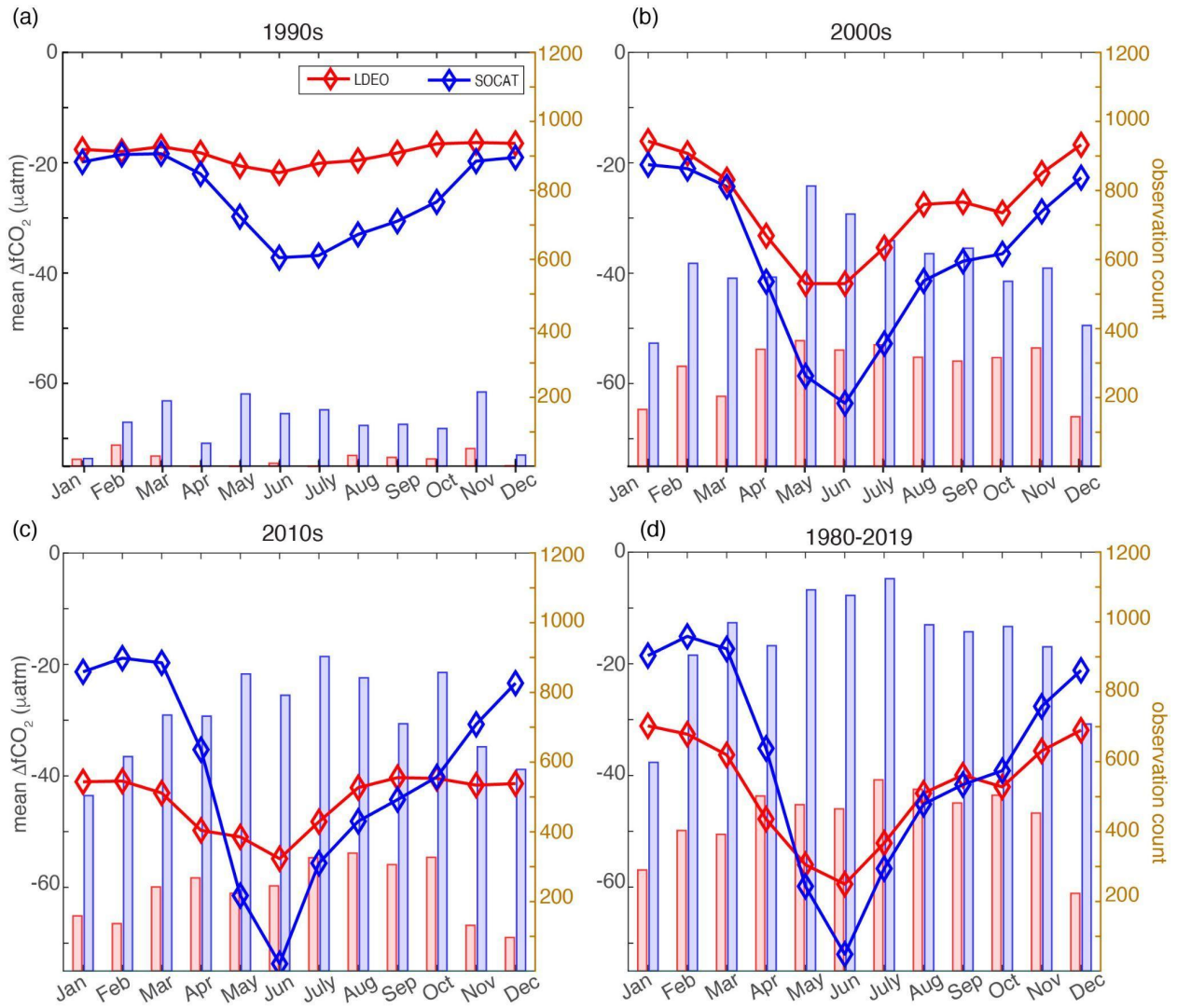
Figure S6: Annual mean difference in $\Delta f\text{CO}_2$ calculated from the SOCAT database using a constant $1.5\mu\text{atm yr}^{-1}$ time normalization minus the current $\Delta f\text{CO}_2$ method.



53
 54 Figure S7: Seasonal sea–air CO₂ flux (mol C m⁻² year⁻¹) climatology for (a) December,
 55 January, February (DJF) and (b) June, July, August (JJA) using the LDEO database.
 56 Positive values (warm colors) indicate sea-to-air fluxes (ocean efflux), and negative
 57 values (cool colors) indicate air-to-sea fluxes (ocean uptake).
 58



59
 60 Figure S8: (a) Annual mean CO₂ flux calculated from the LDEO database and (b)
 61 difference in flux between the SOCAT and LDEO database climatologies (SOCAT
 62 *minus* LDEO). Flux is calculated identically for each climatology, using the SeaFlux
 63 method using the mean of three wind speed reanalysis products. Warm colors indicate
 64 regions of carbon efflux and cool colors indicate regions of carbon uptake. The global
 65 mean flux is -1.79 PgC yr⁻¹ for SOCAT and -1.68 PgC yr⁻¹ for LDEO.
 66
 67



68
 69 Figure S9: Monthly mean values for sea-air $\Delta f\text{CO}_2$ differences in the North Atlantic
 70 Subpolar biome. Average values for each month are plotted for the LDEO database
 71 (red) and the SOCAT database (blue) for each decade: (a) 1990-1999, (b) 2000-2009,
 72 (c) 2010-2019, and also the full common time period (1980-2019). Bar plots on each
 73 subplot show the number of $1^\circ \times 1^\circ$ grid cells in this region which contain observations in
 74 the two databases.

75
 76

77 **Supplementary**

78

79 Here we discuss the method and results based on observations included in the
80 LDEOv2019 database to create an updated climatology. Comparisons are also made to
81 the climatology discussed in the main text which is based on the SOCATv2022
82 database.

83

84 **S1. Methods**

85

86 **S1.1 LDEO database**

87

88 The LDEOv2019 database (available at [https://www.ncei.noaa.gov/access/ocean-](https://www.ncei.noaa.gov/access/ocean-carbon-acidification-data-system/oceans/LDEO_Underway_Database/)
89 [carbon-acidification-data-system/oceans/LDEO_Underway_Database/](https://www.ncei.noaa.gov/access/ocean-carbon-acidification-data-system/oceans/LDEO_Underway_Database/), Takahashi et al.
90 (2020)) consists of over 14 million measurements of $p\text{CO}_2^{\text{oce}}$ with the earliest
91 observations dating back to 1957 and the most recent collected in 2019 (Supplementary
92 Figure 1). This database includes only $p\text{CO}_2^{\text{oce}}$ values measured directly using the air-
93 water equilibration method and requires that two or more standard gas mixtures were
94 used for analyzer calibrations. This strict criteria for observation quality is unique to the
95 LDEO database.

96

97 In this analysis, we restrict the time period to include observations collected beginning in
98 1980, which accounts for 99.9% of the available observations within the LDEOv2019
99 database. Additionally, we eliminate observations in the database that are not
100 accompanied by both an observed sea surface temperature (SST) and atmospheric sea
101 level pressure (SLP). Not only does this act to flag observations that might not be of the
102 highest quality, it also allows a consistent methodology for creating the climatology from
103 both the LDEO and SOCAT databases since the ancillary observations of SST and SLP
104 are necessary to convert from $p\text{CO}_2$ to $f\text{CO}_2$, as well as to calculate a delta value, both
105 steps which are essential in this updated climatology version.

106

107 Within the LDEO database, there are approximately 9400 observations without SST
108 observations and nearly 755,000 missing SLP. Given instances where both SST and
109 SLP are missing, the total number of omitted observations with this criteria is 764,115.
110 Approximately 13.4 of the 14 million observations in the LDEO database meet all
111 ancillary data requirements.

112

113 We have converted all $p\text{CO}_2$ observations in the LDEO database to $f\text{CO}_2$ values. As a
114 pre-processing step, we have calculated $f\text{CO}_2$ values at the reported SST which helps
115 to ensure a uniform representation of the surface ocean observations. The protocol for
116 this conversion step follows that of the SOCAT methodology (Pfeil et al. 2013) which
117 utilizes the equations recommended by Dickson et al. (2007) and requires observed
118 temperature, salinity, and pressure.

119

120 Given the dramatic increase in $p\text{CO}_2^{\text{oce}}$ measurements available since previous
121 releases of the climatology (LDEOv2006, T-2009, and LDEOv2012, T-2014, included
122 nearly 3 and 6.5 million observations, respectively, covering years 1970 to 2007 and

123 1957 to 2012, respectively), we do not remove the observations collected in the
124 equatorial Pacific during El Niño years since inclusion does not strongly influence the
125 overall result as in previous versions where those data made up a larger percentage of
126 available observations.

127
128 There is a large overlap between the LDEO and SOCAT databases particularly for data
129 prior to circa 2015. The LDEO and SOCAT databases are similar in that they restrict the
130 included data to only observations that are measured in near-continuous operation or in
131 discrete samples with an equilibrator system. Neither database includes $p\text{CO}_2/f\text{CO}_2$
132 measurements that are calculated from dissolved inorganic carbon, total alkalinity
133 and/or pH.

134 135 **S1.2 Atmospheric $f\text{CO}_2$ calculation for LDEO database**

136
137 For the LDEO database, the corresponding atmospheric CO_2 value is not included in
138 the reported database as it is in the SOCAT database, so atmospheric CO_2 values from
139 the NOAA MBL product (Lan et al. 2023) are matched based on month and location
140 (latitude) of the $p\text{CO}_2^{\text{oce}}$ observation. In calculating $f\text{CO}_2$ from $p\text{CO}_2$, we use the
141 reported SLP, SST and salinity from the LDEO database.

142 143 **S2. Results**

144 145 **S2.1 LDEO $\Delta f\text{CO}_2$ climatology**

146 147 **S2.1.1 Global**

148
149 Supplementary Figure 2 shows the near-global annual climatological mean distribution
150 of $\Delta f\text{CO}_2$ ($f\text{CO}_2^{\text{oce}}$ minus $f\text{CO}_2^{\text{air}}$) for both databases. Large-scale patterns across the
151 global ocean include the consistent high (positive) $\Delta f\text{CO}_2$ values in the equatorial Pacific
152 where upwelling is a dominant influence, and low (negative) values of $\Delta f\text{CO}_2$ in the
153 North Atlantic physical processes including evaporation (increase salinity) and cooling
154 drive strong uptake of carbon and subduction of surface waters.

155
156 As for SOCAT, the near-global LDEO $\Delta f\text{CO}_2$ climatology curve has a bimodal shape
157 (Supplementary Figure 3) with a smaller peak in boreal spring (March/April) and a larger
158 peak in late boreal summer (August/September). The LDEO curve reaches its minimum
159 in January and begins a recovery throughout the boreal winter before dipping again for
160 a springtime minimum in May. While the overall pattern is similar between the SOCAT
161 and LDEO curves, the LDEO curve has a larger amplitude, reaching a higher peak and
162 lower trough. The near-global LDEO annual mean $\Delta f\text{CO}_2$ value is $-3.9 \mu\text{atm}$.

163 164 **S2.1.2 Regional**

165
166 The equatorial regions of the Pacific and Atlantic oceans have positive $\Delta f\text{CO}_2$ values
167 throughout the annual cycle and little seasonal variability (Supplementary Figure 3,
168 4ab). This indicates that these areas are sources of CO_2 to the atmosphere year round.

169 The equatorial Pacific has the highest positive $\Delta f\text{CO}_2$ values (annual mean of 31.5
170 μatm), followed by the tropical Atlantic (annual mean of 11.6 μatm , Supplementary
171 Figure 4).

172
173 The subtropical biomes, representing the temperate North and South Atlantic and
174 Pacific basins exhibit large seasonal $\Delta f\text{CO}_2$ cycles which change sign throughout the
175 year (Supplementary Figure 4); positive $\Delta f\text{CO}_2$ occurs in warm summer months and
176 negative values in colder winter months reflecting the dominance of seasonal
177 temperature changes on the cycles of $\Delta f\text{CO}_2$ in these regions. In the LDEO database,
178 the seasonal amplitude for the subtropical North Pacific is 43.3 μatm , and is slightly
179 larger than the seasonal amplitude in the subtropical North Atlantic (39.6 μatm). The
180 same pattern is observed in the SOCAT database however with slightly larger
181 amplitudes for both basins (Figure 4, Supplementary Figure 4). Since the mean
182 seasonal amplitudes for SST are quite similar in these two oceans, with the Atlantic
183 having a slightly larger seasonal change in surface temperature (4.4°C in Pacific and
184 5.0°C in Atlantic), the difference in $\Delta f\text{CO}_2$ amplitudes between the Pacific and Atlantic
185 subtropical regions cannot be attributed solely to SST, and may reflect differences in
186 biogeochemical cycling between these two basins.

187
188 Seasonal changes in the northern subtropical oceans are roughly six months out of
189 phase from the southern subtropical biomes. The South Pacific subtropical biome has
190 significantly smaller seasonal amplitude than the corresponding Northern Hemisphere
191 region; the South Pacific subtropical biome amplitude is 15.3 μatm . The amplitude in the
192 South Atlantic subtropical basin is much more comparable to the North Atlantic (South
193 Atlantic subtropical amplitude is 37.1 μatm). The Indian Ocean subtropical biome, which
194 encompasses most of the Indian Ocean, both above and below the Equator, has a
195 smaller amplitude (19.8 μatm) but the phasing matches well with the South Pacific and
196 Atlantic biomes, with peak (positive) $\Delta f\text{CO}_2$ values in February and the lowest values in
197 August (Supplementary Figure 4). The low $f\text{CO}_2$ in the Indian and South Pacific
198 subtropical basin is partially attributable to lower SST variability in these regions (SST
199 seasonal cycle amplitudes are 4.0°C in South Pacific and 3.0°C in the Indian as
200 compared to 4.6°C in the South Atlantic) however it is likely that differences in
201 spatiotemporal patterns of primary productivity also contribute to this difference. The
202 striking difference in the amplitude of the cycle in the South Pacific and Indian
203 subtropics could also be influenced by undersampling in these basins and in the
204 Southern Hemisphere oceans overall.

205
206 The timing of the peak drawdown in the subpolar regions is opposite that observed in
207 the subtropical North Pacific and Atlantic basins. A strong negative $\Delta f\text{CO}_2$ in the spring
208 to summer months is due to the effects of biological drawdown which quickly and
209 dramatically lowers the CO_2 levels of the surface ocean. With its biological dependence
210 and strongly stratified mixed layers, the subpolar region seasonal cycle are roughly four
211 to six months out of phase with those from the adjacent subtropical regions. In the
212 Atlantic subpolar biome, $\Delta f\text{CO}_2$ values are consistently below zero throughout the
213 annual cycle (maximum of -31.1 μatm occurs in January). In the Pacific basin, the
214 ocean exceeds the atmospheric levels of $f\text{CO}_2$ in the boreal winter (Jan-March) before

215 the spring bloom results in biological drawdown which lowers the $\Delta f\text{CO}_2$ values below
216 zero for the remainder of the year. The spring drawdown is weaker in the Pacific basin
217 than the Atlantic.

218
219 Supplementary Figure 4c displays the seasonal cycle for the Southern Ocean biomes
220 including the seasonal ice biome, the subpolar region, and the seasonally stratified
221 subtropical region of the Southern Hemisphere. Unlike the subtropical regions of the
222 other basins, this region has a relatively small seasonal $\Delta f\text{CO}_2$ amplitude and has
223 consistently negative $\Delta f\text{CO}_2$ values (atmosphere>ocean) throughout the annual cycle.
224 The mean of this Southern Ocean subtropical region is $-20.9 \mu\text{atm}$ with a maximum
225 amplitude of $9.1 \mu\text{atm}$.

226
227 Unlike the seasonally-stratified subtropical region of the Southern Ocean, the Southern
228 Ocean subpolar and ice biomes both have relatively strong seasonal cycles, reaching a
229 maximum $\Delta f\text{CO}_2$ of zero or slightly positive during the late austral winter and early
230 austral spring (Supplementary Figure 4).

231

232 **S2.2 LDEO flux**

233

234 The mean annual air-sea CO_2 flux for the LDEO database is $-1.68 \text{ PgC yr}^{-1}$ with
235 negative indicating an uptake by the ocean. This represents a slightly greater flux into
236 the ocean than the direct estimate from the previous version of the climatology
237 (Takahashi et al. 2009) which estimated global mean flux at 1.4 PgC yr^{-1} . For the
238 uncertainty in global ocean-atmosphere CO_2 flux reported here we use the value
239 reported by Wanninkhof et al. (2013) as described above.

240

241 The global mean flux estimate presented here is for the area of the global ocean
242 covered by this database and does not fully extend over the entire global ocean; it
243 covers 90% of the global ocean. Specifically, coastal and high latitude regions are
244 missing also as described above for the SOCAT database.

245

246 Supplementary Figure 7 shows the climatological seasonal mean sea-air CO_2 flux (mol
247 $\text{m}^{-2} \text{ yr}^{-1}$) for two seasons (DJF and JJA). The equatorial Pacific is the most prominent
248 atmospheric CO_2 source region, with a seasonally persistent sea-to-air flux. When
249 combined with the equatorial Atlantic region, the tropical belt emits an annual mean
250 0.35 PgC yr^{-1} to the atmosphere.

251

252 Adjacent to this tropical efflux zone lies an area of seasonally variable uptake patterns.
253 The subtropical basins in both hemispheres act as CO_2 sinks in the cooler months and
254 transition to regions of neutral or small CO_2 sources during the warmer months. At
255 higher subtropical latitudes, strong winds and relatively low ocean $f\text{CO}_2$ occur along the
256 subtropical convergence zone- a region where the cooled subtropical gyre waters with
257 low $f\text{CO}_2$ meet the subpolar waters with biologically-lowered $f\text{CO}_2$.

258

259 The Northern Hemisphere subtropical region represents a smaller sink ($-0.64 \text{ PgC yr}^{-1}$)
260 than the corresponding Southern Hemisphere region ($-0.82 \text{ PgC yr}^{-1}$), largely due to the

261 overall greater size of the oceans in the Southern Hemisphere at these latitudes as
262 noted above. There is also significant uptake in the Southern Ocean subtropical region
263 (-0.55 PgC yr⁻¹).

264

265 **S2.3 Comparison of climatologies built from SOCAT and LDEO databases**

266

267 **S2.3.1 Global**

268

269 On a global scale, the monthly mean $\Delta f\text{CO}_2$ seasonal amplitudes for the climatology
270 produced using the LDEO database is larger than for the SOCAT database, reaching
271 both higher in the boreal summer and lower in the boreal winter months. The LDEO
272 climatology has an amplitude of 6.6 μatm while the SOCAT global mean climatology
273 amplitude is 5.0 μatm (Supplementary Figure 2).

274

275 The mean annual air-sea CO₂ flux resulting from the LDEO version of the climatology
276 created is -1.67 PgC yr⁻¹, with negative value indicating an uptake by the ocean. This
277 represents a slightly greater flux into the ocean than the direct estimate from the
278 previous version of the climatology (T-2009) which estimated global mean flux of -1.4
279 PgC yr⁻¹. This shift towards greater carbon uptake is consistent with other work
280 indicating increased ocean uptake in recent decades (Friedlingstein et al. 2022, DeVries
281 et al. 2023).

282

283 The LDEO climatology annual mean flux is slightly less negative than the mean global
284 air-sea CO₂ flux based on the SOCAT database (-1.79 PgC yr⁻¹). While the overall
285 shape of the seasonal cycle is comparable between the two databases, the amplitude in
286 flux is much larger for the LDEO database, a result of the larger $\Delta f\text{CO}_2$ global mean
287 amplitude (Supplementary Figure 2). Specifically, the LDEO database has global mean
288 flux values approaching zero during the boreal summer months, leading to a reduced
289 uptake of carbon during these months. While the boreal winter months have similar flux
290 estimates between the two databases, the difference during the months of July, August,
291 and September ultimately reduce the overall global mean flux value reported from the
292 LDEO database.

293

294 **S.2.3.2 Southern Ocean**

295

296 While the total annual Southern Ocean (<35S) flux estimates are similar (-1.04 PgC yr⁻¹
297 and -0.90 PgC yr⁻¹ for SOCAT and LDEO respectively), discrete regions of the Southern
298 Ocean exhibit some of the largest differences in the climatological air-sea flux created
299 from the SOCAT versus LDEO database (Figure 5, Supplementary Figure 6).

300 Specifically, in the ocean region south of Australia, the SOCAT database produces flux
301 estimates of larger carbon uptake/less efflux than the LDEO database. This signal of
302 larger uptake estimates in the SOCAT database is consistent throughout all months of
303 the year but peaks during August, September, and October. These differences are likely
304 a result of more available observations in the SOCAT database in this region (Figure 1,
305 Supplementary Figure 1). Throughout the vast expanse of the remainder of the
306 Southern Hemisphere subtropical and subpolar regions (i.e. the Pacific and Atlantic

307 sectors), the differences are much smaller and heterogeneous (Figure 5,
308 Supplementary Figure 6). Therefore, we do not see substantial biome-scale differences
309 in the climatology of either $\Delta f\text{CO}_2$ or carbon flux despite the small anomalous region
310 south of Australia.

311

312 **S2.3.3 North Atlantic Subpolar Differences**

313

314 For most regions of the global ocean, the $\Delta f\text{CO}_2$ climatological cycle is consistent
315 between the SOCAT and LDEO datasets (Figure 4, Supplementary Figure 4).
316 Differences in the absolute magnitude of the $\Delta f\text{CO}_2$ values are also observed in the
317 equatorial regions in both the Atlantic and Pacific basins where SOCAT has slightly
318 larger $\Delta f\text{CO}_2$ values, but the overall shape and amplitude of the seasonal cycle is
319 consistent between the two databases. One exception to this is the North Atlantic
320 subpolar region where the differences in seasonal climatology between the two datasets
321 are large. The North Atlantic subpolar region has similar total annual $\Delta f\text{CO}_2$ estimates (-
322 37.45 μatm and -42.33 μatm for SOCAT and LDEO respectively) but the seasonal
323 differences are profound (Supplementary Figure 9).

324

325 The seasonal amplitude in the North Atlantic subpolar biome is over two times as large
326 for the SOCAT database compared to the LDEO database (28.3 μatm in LDEO and
327 56.9 μatm in SOCAT; Figure 4 and Supplementary Figure 4). While the phasing and
328 shape of the seasonal cycle is consistent between the two databases in this region,
329 there is a significant difference in the amplitude of the winter to summer transition. While
330 the winter (DJF) mean $\Delta f\text{CO}_2$ is about 10 μatm different between the two (LDEO being
331 more negative than SOCAT), the opposite is true for the summer season with the
332 SOCAT showing more positive values. The transition to spring and summer blooms,
333 when $\Delta f\text{CO}_2$ is greatly reduced allowing for more uptake by the surface ocean, is very
334 different between the two databases with a March to June change of 54.7 μatm in the
335 SOCAT database versus 23.1 μatm for LDEO. Spring/Summer (MAM/JJA) $\Delta f\text{CO}_2$
336 values for the LDEO database are -46.7 and -51.6 μatm , respectively, while for the
337 SOCAT database corresponding values are -37.4 and -57.9 μatm , respectively (Figure
338 4, Supplementary Figures 4 and 9). While an annual mean value in this region may not
339 show a significant difference between the two databases, the differences in seasonal
340 cycle amplitude are likely driven by mechanisms that are more completely captured by
341 the higher sampling density of the SOCAT database and missed in LDEO.

342

343 The amplitude of the seasonal cycle increases with time from the 1990s to the 2000s in
344 both databases, however it is the 2010-2019 time period that shows the strongest
345 differences between the climatology produced by each database (Supplementary Figure
346 9). For the most recent decade (2010-2019), the amplitude of $\Delta f\text{CO}_2$ calculated from the
347 LDEO database actually decreases from the previous decade (14.6 μatm) while the
348 amplitude from the SOCAT database is larger than any previous decade, exceeding 50
349 μatm in absolute amplitude (SOCAT amplitude is 54.8 μatm ; Supplementary Figure 9c).
350 The LDEO database is likely lacking sufficient seasonal observations to fully capture the
351 biological drawdown that characterizes this region.

352

353 Specifically, this stark contrast is likely due to the abundance of observations in the
354 higher latitudes of the North Atlantic subpolar region in the SOCAT database around
355 Iceland and extending into the Norwegian Sea (Figure 1, Supplementary Figure 1). This
356 result is due both to differences in spatial and temporal coverage. Many grid cells in the
357 version created from the SOCAT database include full seasonal coverage (twelve
358 unique months of observations over the full time period considered). This subpolar
359 North Atlantic is a very dynamic region particularly over the spring/summer months with
360 strong biological drawdown of CO₂ in strongly stratified shallow mixed layers. In order to
361 accurately capture the seasonal evolution of $\Delta f\text{CO}_2$, it is imperative to have
362 observations from each season. To capture the evolution of the seasonal cycle in this
363 region over long time intervals requires near continuous full seasonal coverage of
364 observations highlighting the importance of expanded efforts to observe the high
365 latitude oceans.

366

367

368 Supplementary References

369

370 Takahashi, Taro; Sutherland, Stewart C.; Kozyr, Alex (2020). Global Ocean Surface
371 Water Partial Pressure of CO₂ Database: Measurements Performed During 1957-2019
372 (LDEO Database Version 2019) (NCEI Accession 0160492). Version 9.9. NOAA
373 National Centers for Environmental Information. Dataset.
374 [https://doi.org/10.3334/CDIAC/OTG.NDP088\(V2015\)](https://doi.org/10.3334/CDIAC/OTG.NDP088(V2015))

375